

Dynamical effects on the way to fusion of very heavy nuclei

I.N. Mikhailov^{1,3,a}, T.I. Mikhailova², Ch. Briançon³, and F. Hanappe⁴

¹ Bogoliubov Laboratory of Theoretical Physics, JINR, Dubna, Russia

² Dzhelapov Laboratory of Nuclear Problems, JINR, Dubna, Russia

³ CSNSM (IN2P3-CNRS), Orsay, France

⁴ ULB, Bruxelles, Belgium

Received: 4 October 2005 / Revised: 3 May 2006 /

Published online: 26 June 2006 – © Società Italiana di Fisica / Springer-Verlag 2006

Communicated by W. Henning

Abstract. The central collision of ^{40}Ar and ^{208}Pb is studied considering the ellipsoidal deformations and isovector dipole mode of motion in the approaching phase. The collective energy dissipation is suggested to originate from the Fermi surface deformation which is treated as a kinematically independent mode of motion within the canonical Lagrange-Rayleigh dynamics. The possible extensions of the approach are discussed. The potential energy surface, calculated using the generalized (folded) surface potential, is studied. The saddle point in the potential energy surface lying at the border of strongly deformed compact configurations is located. The potential energy at this point is about 10 MeV smaller than that of the ions touching each other in the spherical shape. The examination of trajectories followed by the system in its evolution shows that the inertia forces strongly hinder the motion of ions along the potential energy valley. The collective energy dissipated during the approach is found to be smaller than the difference in the potential energies at saddle point and at the touching configuration of unpolarized ions.

PACS. 24.10.-i Nuclear reaction models and methods – 25.70.Jj Fusion and fusion-fission reactions

1 Introduction

The recent experiments aiming at the production of very heavy and super-heavy nuclei have revived the interest in establishing the conditions for the heavy-ion fusion [1]. Such conditions have been explored for a long time (with much success for not excessively heavy ions) by many physicists and, in particular, in a series of papers included in ref. [2]. In these studies it was found that the most important circumstance making fusion possible for the two colliding nuclei is provided by the passage beyond the saddle point in the potential energy surface of the nucleus which may be produced in the collision.

The conditions for fusion must be looked for in the dynamics of the collision and depend on the inertial properties and on the potential forces of the system. The other important element lies in the coupling between the collective and intrinsic degrees of freedom responsible for the collective energy dissipation. This coupling plays a very important role in the fusion reaction. Indeed, the fusion takes place when the initial kinetic energy of approaching ions is shared between numerous intrinsic degrees of freedom, *i.e.* is dissipated. The coupling of collective modes

between themselves and with the intrinsic degrees of freedom produces different effects depending on the duration of the process. The rate of the energy dissipation in the fast changes of configuration differs much from the dissipation rate when the evolution is slow. In other words the “memory” properties of nuclear systems are also of importance.

With the increasing Z -number of the nucleus, which is expected to be produced in the collision, the Coulomb repulsion pushes the potential energy ridge outside of the space of compact forms with overlapping densities of the collision partners. Then, the possibility of overcoming the ridge becomes dependent on the configuration attained by the colliding nuclei just before establishing the contact. Thus, the description of very heavy-nuclei formation demands the knowledge of dynamical effects taking place before the unification of ions. The Coulomb repulsion flattens the potential energy surface inside the ridge. For this reason, the conditions for the fusion of very heavy nuclei at lowest incident energies and small values of angular momentum are of special interest. These conditions are discussed in this paper taking as an example the $^{40}\text{Ar} + ^{208}\text{Pb}$ central collision. We study here the role of the inertia properties of ions and the energy dissipated via the excitation of the quadrupole and dipole

^a e-mail: mikhailo@csnsm.in2p3.fr

degrees of freedom. The role of the “memory effects” in slowing down the information passing from one degree of freedom to another one is examined. The study reported here is done within the approach of refs. [3–5]. This approach is presented here in a new and more transparent way and is generalized for the description of collisions in non-symmetrical systems and includes the participation of the isovector dipole modes of motion.

The composition of the paper is as follows:

- In sect. 2 the collective variables and the equations of motion describing the evolution of approaching ions are presented. The ellipsoidal deformations of approaching ions and the isovector dipole mode of motion within them are included in the collective space. The collective energy dissipation is considered to originate from the quadrupole deformation of the Fermi surface of ions, which is considered as being kinematically independent from the other modes of motion. The evolution of collective variables is of the type of the Lagrange-Rayleigh classical mechanics which makes possible the definition in an unambiguous way of the collective energy and its dissipation rate.
- In sect. 3 we examine the potential energy surface using the generalized (folded) surface potential. The 3-dimensional potential energy surface exhibits a “ridge” within the configuration space describing the motion of separated ions and the saddle point corresponding to strongly deformed ions in compact configurations. The saddle point is situated very near the border of the compact configuration space.
- In sect. 4 the trajectories of the system of approaching ions in the configuration space of the model are examined. The role of the inertia properties of ions is studied. The notion of a “separatrix” trajectory is introduced. The evolution along this trajectory leads to the saddle point where an unstable equilibrium of the nucleus-nucleus interaction forces is established.
- In sect. 5 the energy dissipation occurring during the approach is considered. It is found that, at the minimal incident energy of collision at which the contact between the ions is realized, the dissipated collective energy is smaller than the difference of the potential energies in the saddle point and in the configuration of two “unpolarized” (spherical) ions at the contact. The role of the “retardation” effects in establishing the sufficient conditions for fusion is briefly discussed.
- In sect. 6 a recapitulation of the results of the study is presented.
- Two appendices follow the main text with the discussion of the quantum-mechanical substratum of the Lagrangian (appendix A) and of different dissipation mechanisms (appendix B).

2 Equations of motion

The approaching ions are considered as droplets of incompressible nuclear matter homogeneously distributed within

a sharp surface. In the ground states, the ions are supposed to have spherical shape and zero value of the angular momentum. The center of mass of the nuclear system coincides with the origin of the coordinates frame having the z -axis coincident with the direction of ions motion. Consistently with these suggestions, the ions keep the axial symmetry during their evolution with their symmetry axes remaining coincident with the z -axis of the reference frame. We strengthen these suggestions assuming the spheroidal shape of ions. The instantaneous values of the semi-axes of an ion “number i ” $a_k^{(i)}(t)$, ($i = 1$ or 2—the ion’s number, $k = x, y, z$ -indexes of the coordinates axes) will be related with the parameter η_i as follows

$$a_x^{(i)} = a_y^{(i)} \equiv a_{\perp}^{(i)} = R_i \eta_i, \quad a_z^{(i)} \equiv a_{\parallel}^{(i)} = R_i / \eta_i^2, \\ \text{where} \quad R_i = r_0 A_i^{1/3} \quad (r_0 = 1.18 \text{ fm}) \quad (1)$$

(here R_i is the global radius of the ion in its ground state; in the following we shall use an equivalent deformation parameter $\alpha_i = 1 - \eta_i$).

2.1 Elastoplastic model

The dynamics of approaching ions is described by the evolution of the elongation parameter $L(t)$ (the distance between the centers of mass of the ions) and by the intrinsic quadrupole moments of the ions $q_i(t)$. These quantities are defined as follows

$$L(t) = |L_1(t) - L_2(t)|, \quad (2)$$

$$L_i(t) = \frac{1}{A_i} \int_{V_i} d\mathbf{x} z n(\mathbf{x}, t), \quad (3)$$

$$q_i(t) = m \int_{V_i} d\mathbf{x} [2(z - L_i)^2 - x^2 - y^2] n(\mathbf{x}, t). \quad (4)$$

Here L_i is the z -coordinate of the center of mass and A_i is the number of nucleons in each of the two ions. Further, m is the nucleon mass, $n(\mathbf{x}, t)$ is the particle density and the integration goes over the volume V_i of the ion.

Equations determining the evolution of these variables are obtained on the basis of virial theorems¹ integrating with appropriate weights the kinetic equation for the Wigner transform [10] of the one-body density matrix

$$\langle \mathbf{x}_1; \sigma_1, \nu_1 | \hat{\rho}(t) | \mathbf{x}_2; \sigma_2, \nu_2 \rangle$$

(see, *e.g.*, ref. [11]). The relation between the Wigner transform ($f(\mathbf{p}, \mathbf{x}, t)$) and the density matrix (summed over the nucleonic spin-isospin indexes in the study of the

¹ The method of virial theorems for solving the hydrodynamical equations was introduced by S. Chandrasekhar [6]. The references to its applications for the nuclear problem studies may be found in [7] or in the earlier published review papers [8] and [9] containing essentially the same material.

isoscalar modes of motion) reads

$$f(\mathbf{p}, \mathbf{x}, t) = \frac{1}{(2\pi\hbar)^3} \int d\mathbf{s} e^{-i\mathbf{p}\cdot\mathbf{s}/\hbar} \sum_{\sigma,\nu} \left\langle \mathbf{x} + \frac{\mathbf{s}}{2}; \sigma, \nu \mid \hat{\rho}(t) \mid \mathbf{x} - \frac{\mathbf{s}}{2}; \sigma, \nu \right\rangle. \quad (5)$$

In this relation $\sigma = \pm 1$ ($\nu = \pm 1$) have twice the value of the spin (isospin) quantum number of the single-particle state contributing to the density matrix. The Wigner transform of the density matrix allows to determine the mean value of any function depending on the coordinates (\mathbf{x}) and the linear momentum (\mathbf{p}) of a nucleon.

The kinetic equation is

$$\begin{aligned} & \frac{\partial f(\mathbf{p}, \mathbf{x}, t)}{\partial t} + \frac{\mathbf{p}}{m} \cdot \nabla_{\mathbf{x}} f(\mathbf{p}, \mathbf{x}, t) \\ & - \frac{2}{\hbar} \sin\left(\frac{\hbar}{2} \nabla_{\mathbf{x}}^{(U)} \cdot \nabla_{\mathbf{p}}^{(f)}\right) U(\mathbf{x}, t) f(\mathbf{p}, \mathbf{x}, t) \\ & = -I_{\text{cls}}(\mathbf{p}) \end{aligned} \quad (6)$$

Here $\nabla_{\mathbf{x}}^{(U)}$ ($\nabla_{\mathbf{p}}^{(f)}$) are the gradient operators differentiating, respectively, in the space of coordinates \mathbf{x} and in the space of linear momenta \mathbf{p} . The first of them operates on the potential function $U(\mathbf{x}, t)$ and the second on the Wigner function $f(\mathbf{p}, \mathbf{x}, t)$.

The left-hand side of this equation contains the terms corresponding to the time-dependent Hartree-Fock theory and describes the independent motion of nucleons in the mean field. On the right-hand side of it appears the Wigner transform of the so-called ‘‘correlation term’’ present in the equation for the one-body density matrix, the term responsible for mixing of many-body configurations. In the equation for the $f(\mathbf{p}, \mathbf{x}, t)$ -function this term appears under the guise of the ‘‘collision integral’’ $I_{\text{cls}}(\mathbf{p})$ of the classical kinetic theory and describes the dissipation of the collective energy followed by its transformation in the statistical excitation energy. In the case of an homogeneous distribution of the matter inside the ions this quantity must be position independent and satisfies the conditions known in the classical kinetic theory [12,13]:

$$\int d\mathbf{p} I_{\text{cls}}(\mathbf{p}) = \int d\mathbf{p} \mathbf{p} I_{\text{cls}}(\mathbf{p}) = 0, \quad (7)$$

$$\int d\mathbf{p} \mathbf{p}^2 I_{\text{cls}}(\mathbf{p}) = 0, \quad (8)$$

otherwise the conservation rules of the basic invariants (particle number, total linear and angular momenta and the total energy) would be violated.

The integration of $f(\mathbf{p}, \mathbf{x}, t)$ goes first over the linear momenta giving rise to relations between the quantities appearing in the classical description of extended systems and called ‘‘attributes’’ of the nuclear-matter elements. The following attributes are of importance in this work:

- the nuclear particle and matter densities:

$$\rho(\mathbf{x}, t) = m n(\mathbf{x}, t) = m \int d\mathbf{p} f(\mathbf{p}, \mathbf{x}, t),$$

- the components of the collective velocity field:

$$\mathbf{u}_i(\mathbf{x}, t) = (1/\rho) \int d\mathbf{p} \mathbf{p} f(\mathbf{p}, \mathbf{x}, t),$$

- and the pressure tensor:

$$P_{i,j}(\mathbf{x}, t) = (1/m) \int d\mathbf{p} (p_i - mu_i)(p_j - mu_j) f(\mathbf{p}, \mathbf{x}, t).$$

The first step of integration establishes relations between the attributes of the nuclear-matter elements involving the well-known continuity equation and the other equations which can be found in the references quoted in the footnote¹.

The next step in arriving at virial theorems consists in integrating in the position coordinates the equations obtained in the first step. This integration leads to the dynamical equations of motion for the collective variables in eqs. (3) and (4):

$$\mu \frac{d^2 L}{dt^2} = -\frac{\partial U(L, q_1, q_2)}{\partial L}, \quad (9)$$

$$\frac{1}{2} \ddot{q}_i = \kappa_i(q_i) \dot{q}_i^2 - w_i(L, q_1, q_2) + \pi_i, \quad (10)$$

In these equations $\mu = m(A_1 \cdot A_2)/(A_1 + A_2)$ is the reduced mass of the two ions. The quantity

$$U(L, q_1, q_2) = \int_{V_1+V_2} d\mathbf{x} W(\mathbf{x}, t) n(\mathbf{x}, t) \quad (11)$$

is the common collective potential determined by the local mean-field potential $W(\mathbf{x}, t)$ including the Coulomb and nuclear interactions between the ions and within them. Its properties and those of the function

$$w_i = \int_{V_i} d\mathbf{x} \left(2z \frac{\partial W}{\partial z} - x \frac{\partial W}{\partial x} - y \frac{\partial W}{\partial y} \right) n(\mathbf{x}, t) \quad (12)$$

will be discussed in the next section.

The velocity \mathbf{u}_i determines the kinetic energy of collective flow within the ions ($T_{q_i}^{\text{coll}} = m_i(q_i) \dot{q}_i^2/2$) via the effective mass parameter $m_i(q_i)$ and the function

$$\kappa_i(q_i) = \frac{1}{\dot{q}_i^2} \int_{V_i} d\mathbf{x} \left[2u_{\parallel}^2 - \mathbf{u}_{\perp}^2 \right]_i n(\mathbf{x}, t) \quad (13)$$

$u_{\parallel}(\mathbf{x}, t) = u_z(\mathbf{x}, t)$ and $\mathbf{u}_{\perp}(\mathbf{x}, t) = u_x(\mathbf{x}, t)\mathbf{e}_x + u_y(\mathbf{x}, t)\mathbf{e}_y$; \mathbf{e}_k being the unit vectors of the reference frame.

Equation (10) contains the quantity

$$\pi_i(t) = 2 \int_{V_i} d\mathbf{x} [P_{\parallel}(\mathbf{x}, t) - P_{\perp}(\mathbf{x}, t)] \quad (14)$$

($P_{\parallel}(\mathbf{x}, t) = P_{z,z}(\mathbf{x}, t)$, $P_{\perp}(\mathbf{x}, t) = (P_{x,x}(\mathbf{x}, t) + P_{y,y}(\mathbf{x}, t))/2$).

The evolution of this function, as found from the virial theorems method, is given by

$$\begin{aligned} & \dot{\pi}_i + 2 \int_{V_i} d\mathbf{x} \left(2 \frac{\partial u_z}{\partial z} P_{\parallel}(\mathbf{x}, t) \right. \\ & \left. - \left[\frac{\partial u_x}{\partial x} P_{x,x}(\mathbf{x}, t) + \frac{\partial u_y}{\partial y} P_{y,y}(\mathbf{x}, t) \right] \right)_i = -\frac{\pi_i}{\tau_i}. \end{aligned} \quad (15)$$

On the right-hand side of eq. (15) appears the quantity $-\pi_i/\tau_i$ which is the collision integral $I_{\text{cls}}(\mathbf{p})$ integrated over the volume of an ion and treated in the mean relaxation time approximation. Note that the collision integral does not contribute to the dynamical equations for L and q_i variables²: this property is a consequence of eqs. (7).

The velocity field $\mathbf{u}_i(\mathbf{x}, t)$, the mass parameter $m_i(q_i)$ and the function $\kappa_i(q_i)$ are calculated as in ref. [5] assuming the simplest (linear in coordinates) expression which is consistent with the assumption on the spheroidal shape of ions:

$$\mathbf{u}_i(\mathbf{x}, t) = C_{\parallel}^i(t) z \mathbf{e}_z + C_{\perp}^i(t) (x \mathbf{e}_x + y \mathbf{e}_y). \quad (16)$$

The position-independent functions $C_{\parallel}^i(t)$ and $C_{\perp}^i(t)$ are found from the relation [6]

$$\dot{q}_i = \int_{V_i} d\mathbf{x} \rho_i(\mathbf{x}, t) (\mathbf{u}_i \cdot \nabla) (2(z - L_i)^2 - x^2 - y^2)$$

taking into account the incompressibility of the nuclear matter ($\text{div } \mathbf{u}_i = 0$) and the axial symmetry of the system. One has

$$\begin{aligned} \left(\frac{\partial u_z}{\partial z} \right)_i &= C_{\parallel}(t) = 4\dot{q}_i m_i(q_i), \\ \left(\frac{\partial u_x}{\partial x} \right)_i &= \left(\frac{\partial u_y}{\partial y} \right)_i = C_{\perp}(t) = -2\dot{q}_i m_i(q_i). \end{aligned} \quad (17)$$

The relations between the functions depending on the velocity field read

$$m_i(q_i) = \frac{5}{8mR_i^2 A_i} \frac{1}{\eta_i^2 (1 + 2/\eta_i^6)}, \quad (18)$$

$$\kappa_i(q_i) = -\frac{5}{8mA_i R_i^2} \frac{1 - 4/\eta_i^6}{\eta_i^2 (1 + 2/\eta_i^6)^2}, \quad (19)$$

where η_i is the deformation parameter introduced in eq. (1) and related with the quadrupole moment q_i as

$$q_i = \frac{2}{5} m R_i^2 A_i \left(\frac{1}{\eta_i^4} - \eta_i^2 \right). \quad (20)$$

Using eqs. (17), (18) and (19), one obtains the following expressions for the functions w_i and κ_i :

$$\begin{aligned} w_i(L, q_1, q_2) &= \frac{1}{2m_i(q_i)} \left(\frac{\partial U(L, q_1, q_2)}{\partial q_i} \right), \\ \kappa_i(q_i) &= -\frac{dm_i(q_i)/dq_i}{4m_i(q_i)}. \end{aligned} \quad (21)$$

Taking into account eq. (17) and defining the components of the pressure tensor integrated over the volume as

$$\overline{\Pi_{z,z}^i} \equiv \Pi_{\parallel}^i \quad \text{and} \quad \overline{\Pi_{x,x}^i} = \overline{\Pi_{y,y}^i} \equiv \Pi_{\perp}^i, \quad (22)$$

² Note also that the Planck constant \hbar does not appear explicitly in the obtained relations. However, the quantum background of the approach is not affected by the transformations of the equation for the density matrix (see also appendix A).

one arrives at the following form of eq. (15):

$$\dot{\pi}_i = - \left[8m_i(q_i) \left(2\Pi_{\parallel} + \Pi_{\perp} \right)_i \dot{q}_i + \frac{1}{\tau_i} \pi_i \right]. \quad (23)$$

The quantities $\Pi_{\parallel}^{(i)}$ and $\Pi_{\perp}^{(i)}$ enter in the expression for the kinetic (Fermi) energy of intrinsic motion [8]. Estimated on the basis of the Fermi-gas model (at zero value of the nuclear ‘‘temperature’’ (see appendix A), they are

$$\begin{aligned} \Pi_{\parallel}^{(i)} &= \frac{2}{3} \mathcal{E}_i^{(0)} \left[1 + \frac{1}{2} \frac{\pi_i}{\mathcal{E}_i^{(0)}} + \frac{1}{16} \left(\frac{\pi_i}{\mathcal{E}_i^{(0)}} \right)^2 + \dots \right], \\ \Pi_{\perp}^{(i)} &= \frac{2}{3} \mathcal{E}_i^{(0)} \left[1 - \frac{1}{4} \frac{\pi_i}{\mathcal{E}_i^{(0)}} + \frac{1}{16} \left(\frac{\pi_i}{\mathcal{E}_i^{(0)}} \right)^2 + \dots \right], \end{aligned} \quad (24)$$

where $\mathcal{E}_i^{(0)} = 3mv_F^2 A_i/10$ is the zero-point kinetic energy (v_F being the nucleon’s velocity on the Fermi surface) and (\dots) stands for the terms of higher orders in $(\pi_i/\mathcal{E}_i^{(0)})$.

In eqs. (24) the π_i -independent terms are dominant. This justifies the approximation in which one retains only the terms up to $(\pi_i/\mathcal{E}_i^{(0)})^2$ in the kinetic energy of intrinsic motion expression

$$T_i^{\text{intr}} = \frac{1}{2} \left(\Pi_{\parallel} + 2\Pi_{\perp} \right)_i = \mathcal{E}_i^{(0)} + \frac{\pi_i^2}{16\mathcal{E}_i^{(0)}} \quad (25)$$

and only the first (π_i -independent) term in the combination of Π_{\parallel} and Π_{\perp} functions appearing in eq. (23). Then one obtains:

– the expression for the energy of collective motion:

$$\begin{aligned} \mathcal{E}_i^{\text{coll}} &\equiv \mathcal{E}_i - \mathcal{E}_i^{(0)} \\ &= \frac{\mu}{2} \dot{L}^2 + \sum_{i=1,2} (T_{q_i} + T_{\pi_i}^{\text{coll}}) + U(L, q_1, q_2), \end{aligned} \quad (26)$$

where

$$T_{\pi_i}^{\text{coll}} = \frac{\pi_i^2}{16\mathcal{E}_i^{(0)}}, \quad (27)$$

– and the simplified form of eq. (23):

$$\dot{\pi}_i + \mathcal{F}_i(q_i) \dot{q}_i = -\frac{1}{\tau_i} \pi_i, \quad (28)$$

where $\mathcal{F}_i(q_i) = 16 m_i(q_i) \mathcal{E}_i^{(0)}$.

Retaining only the dependence on L and q_i in the potential function U one arrives at the closed set of equations for the collective variables $L(t)$, $q_i(t)$ and for the quantities $\pi_i(t)$. The set includes eq. (9), eq. (28) and the equation

$$\frac{d}{dt} (m_i(q_i) \dot{q}_i) = -\frac{\partial U}{\partial q_i} + m_i(q_i) \pi_i, \quad (29)$$

The equations of motion (9), (28) and (29) may be cast into the Lagrange-Rayleigh form [4] associating $\pi_i(t)$ with

the time derivative of an “intrinsic collective variable”, *i.e.* assuming that $\pi_i(t) = \dot{\zeta}_i(t)$. It means that the equations of motion and the expression for the collective energy may be written as [14]

$$\frac{d}{dt} \frac{\partial \mathcal{L}}{\partial \dot{Q}_n} - \frac{\partial \mathcal{L}}{\partial Q_n} = - \frac{\partial \mathcal{R}}{\partial \dot{Q}_n}, \quad (30)$$

$$\sum_n \dot{Q}_n \frac{\partial \mathcal{L}}{\partial \dot{Q}_n} - \mathcal{L} = \mathcal{E}_{\text{coll}}. \quad (31)$$

Here \mathcal{L} and \mathcal{R} are, respectively, the Lagrangian and the Rayleigh dissipation function depending on the generalized collective coordinates Q_n and velocities \dot{Q}_n .

The Lagrangian may be easily established noticing that the expression for the energy containing the sum of kinetic and potential energies determines it up to terms linear in generalized velocities [14]. Noticing also that the coupling between the q_i and π_i variables is represented by expressions linear in $\dot{\zeta}_i$, one includes in the Lagrangian the difference of the kinetic and potential energies and adds to it coupling terms linear in $\dot{\zeta}_i$. Then one finds the Lagrangian and Rayleigh functions, which are consistent both with the equations of motion for L , q_i and π_i and with the expression for the collective energy in eq. (26):

$$\mathcal{L}_{\text{quad}} = \frac{\mu \dot{L}^2}{2} + \sum_{i=1,2} \mathcal{T}_i - U(L, q_1, q_2), \quad (32)$$

$$\mathcal{R}_{\text{quad}} = \sum_{i=1,2} \mathcal{R}_i^{\text{quad}} \equiv \sum_{i=1,2} \frac{\dot{\zeta}_i^2}{16\tau_i \mathcal{E}_i^{(0)}}. \quad (33)$$

In the Lagrangian the first term is the kinetic energy of the relative motion of ions, while the second term

$$\mathcal{T}_i = \frac{m_i(q_i)}{2} \dot{q}_i^2 + \frac{\dot{\zeta}_i^2}{16\mathcal{E}_i^{(0)}} + 2\dot{\zeta}_i \int_0^{q_i} m_i(q') dq' \quad (34)$$

includes the kinetic energies of collective flow $T_{q_i}^{\text{coll}}$, collective parts of the intrinsic kinetic energy $T_{\pi_i}^{\text{coll}}$ and the functions describing the coupling of deformations in the coordinate and momentum sectors of the phase space of the ions.

The canonical formulation of the dynamics allows to define in an unambiguous way the dissipation rate of the collective energy:

$$\frac{d\mathcal{E}_{\text{coll}}}{dt} = - \frac{d\mathcal{E}_{\text{stat}}}{dt} = -2\mathcal{R}. \quad (35)$$

In the considered case the dissipation function $\mathcal{R} = \mathcal{R}_{\text{quad}}$ is defined as in eq. (33).

The nature of the “collective part of the intrinsic kinetic energy” and the time scale of the memory effects can be seen noticing that in isolated nuclei and in colliding ions at large distances eqs. (28), (29) describe the properties of the Giant Quadrupole Resonance (GQR): the position of its centroid and its spreading width [15, 8]. These GQR parameters are associated with the real and

imaginary parts of the frequency of small-amplitude time-dependent shape variations around some fixed (or slowly varying with the time) value of q_i^{mean} . The frequency of these vibrations (ω_i^{GQR}) is related to the quantity $\mathcal{F}_i(q_i)$ defined in eq. (28):

$$\omega_i^{\text{GQR}} \approx \sqrt{2\mathcal{F}_i(q_i)} = \sqrt{2} \frac{v_F}{R_i} \sqrt{\frac{m_i(q_i)}{m_i(0)}}$$

showing that its inverse is of the order of the time passed by a nucleon between its collisions with the ion surface. The spreading width of GQR corresponds to the decay of vibrations involved in it during a time about 2–3 times larger.

2.2 Isovector dipole mode participation

The Coulomb interaction of an ion (ion “number i ”) with the electromagnetic field produced by its reaction partner (ion “number j ”) adds to the energy of the i -th ion a term $\mathcal{E}_i^{\text{dip}} = -\mathbf{E}_j \mathbf{d}_i$, where $\mathbf{E}_j = -eZ_j \mathbf{L}/L^3$ is the electric field intensity at the center of mass of the ion “number i ” and \mathbf{d}_i is its electric dipole moment. The effects of this interaction may be estimated in a simple way using the information on the nuclear response to the dipole component of the electromagnetic field. Atomic nuclei respond to it as damped harmonic oscillators, with the effective mass D_i^{dip} and strength parameters C_i^{dip} corresponding to dipole vibrations. These parameters can be related with the sum rule of dipole electric excitations and the centroid of excitation energy of the Giant Dipole Resonance (GDR) [16]:

$$D_i^{\text{dip}} = \frac{A_i}{N_i Z_i} m; \quad C_i^{\text{dip}} = (\omega_i^{\text{GDR}})^2 D_i^{\text{dip}}.$$

When $A \geq 100$ the centroid of excitation energies of GDR states satisfies an empirical rule:

$$\hbar\omega_i^{\text{GDR}} \equiv \hbar(C_i^{\text{dip}}/D_i^{\text{dip}})^{1/2} \approx 79 A_i^{-1/3} \text{ MeV}.$$

In heavy nuclei Γ_i^{GDR} is typically equal to 5 MeV.

The spreading width of GDR may be interpreted in terms of viscosity β_i^{GDR} ($\Gamma_i^{\text{GDR}} \equiv \hbar \beta_i^{\text{GDR}}$). Then, the dynamical equation describing the dipole mode excitation reads

$$D_i^{\text{dip}} \left(\ddot{\mathbf{d}}_i + \frac{C_i^{\text{dip}}}{D_i^{\text{dip}}} \mathbf{d}_i + \beta_i^{\text{GDR}} \dot{\mathbf{d}}_i \right) = e^2 Z_j \mathbf{L}/L^3 \quad (36)$$

and corresponds to the Lagrange-Rayleigh dynamics³ with

$$\begin{aligned}\mathcal{L}^{\text{dip}} &= \sum_i \mathcal{L}_i^{\text{dip}}, \\ \mathcal{L}_i^{\text{dip}} &= \frac{D_i^{\text{dip}}}{2} \dot{\mathbf{d}}_i^2 - \frac{C_i^{\text{dip}}}{2} \mathbf{d}_i^2 + e^2 Z_j \mathbf{L} \cdot \mathbf{d}_i / L^3, \\ \mathcal{R}^{\text{dip}} &= \frac{1}{2} \sum_i D_i^{\text{dip}} \beta_i^{\text{dip}} \dot{\mathbf{d}}_i^2.\end{aligned}\quad (37)$$

2.3 Viscous limit

The evolution of the quantities π_i contributes to the forces restoring the equilibrium shape of the ions. The strength of such forces and their character depend much on the speed of the deformation changes: they show themselves as elastic forces when the shape variations are fast, and are at the origin of the “viscous” behavior of the nuclear matter when the evolution of the shape is slow compared with τ_i . In this case the time derivative of π_i in eq. (28) may be neglected so that the evolution of the system is described by eqs. (9) and (29) with

$$\pi_i = -16\tau_i \mathcal{E}_i^{(0)} m_i(q_i) \dot{q}_i. \quad (38)$$

In this approximation, which we call “viscous”, the equations of motion change their outlook: their number is reduced and, in the equation for the second time derivative of $q_i(t)$, appears a term proportional to \dot{q}_i . This gives to this equation an expressly time-irreversible form. Further, the time derivative of the collective energy as given by eq. (35) becomes proportional to the square of \dot{q}_i functions. To keep the canonical form of the new equations of motion the definition of the Lagrangian and Rayleigh function must be changed: the quantities π_i should be taken out from eq. (32) for the Lagrangian (and from eq. (26) for the collective energy) and be placed in the new Rayleigh function. Equation (35) for the energy dissipation remains valid after changing $\mathcal{R}_{\text{quad}}$ for $\mathcal{R}_{\text{quad}}^{\text{visc}}$ which becomes

$$\mathcal{R}_{\text{quad}}^{\text{visc}} = \frac{1}{2} \sum_{i=1,2} \beta_i^{\text{visc}} (m_i(q_i) \dot{q}_i^2) \quad (39)$$

with

$$\beta_i^{\text{visc}} = 16\tau_i \mathcal{E}_i^{(0)} m_i(q_i).$$

Considering the combined effect of dipole and quadrupole degrees of freedom we write

$$\frac{d\mathcal{E}_{\text{coll}}^{\text{visc}}}{dt} = - \sum_i \left[\beta_i^{\text{visc}} m_i(q_i) \dot{q}_i^2 + \beta_i^{\text{dip}} D_i^{\text{dip}} \dot{\mathbf{d}}_i^2 \right]. \quad (40)$$

When the distribution of the matter within the ions becomes frozen ($\dot{q}_i = \dot{\mathbf{d}}_i = 0$), the collective energy is

³ The invariance properties of collision integral do not concern the dissipative properties of the isovector modes of motion. The structure of eqs. (36) and (37) is similar to that describing the energy dissipation by the quadrupole deformation of ions in the “viscous” approximation (see below).

conserved. It is so, because the variations of the kinetic energy of the relative motion become exactly compensated by those of the potential energy.

The mean relaxation time parameter τ_i appearing in eq. (28) is parameterized as

$$\tau_i = \xi \left(\frac{4}{3} \right)^2 \left(\frac{r_0 A_i^{1/3}}{v_F} \right). \quad (41)$$

The value $\xi = 1$ corresponds to simple arguments formulated in ref. [8], where it is found that with this choice for τ_i the spreading widths of GQR are reasonably well reproduced. Then β_i^{visc} is close to the wall-formula friction parameter β_i^{wall} . At small deformations [17]:

$$\beta_i^{\text{wall}} = \frac{3}{2} \frac{v_F}{r_0 A_i^{1/3}} \quad \text{and} \quad \beta_i^{\text{visc}} = \xi \frac{1}{2} \left(\frac{4}{3} \right)^3 \beta_i^{\text{wall}}. \quad (42)$$

A better reproduction of experimentally found spreading widths of GQR [18] is achieved taking ξ somewhat bigger than 1. This would lead to a bigger difference between β_i^{visc} and β_i^{wall} .

In most of publications concerning the fusion, β_i^{wall} serves as a guide for learning the role of friction (admitting sometimes the necessity of its re-normalization). For this reason we have made most of our calculations taking $\xi = 1$ in order to be reasonably close to the experimentally found properties of giant resonances and not to be too far from the wall formula for friction in the limit of slow changes of the shape. The results of calculations will correspond to this choice of ξ when not stated otherwise. A short discussion on the nature of this parameter is presented in appendix B.

3 Potential function

The potential

$$U(L, q_1, q_2) = U_{\text{folded}}(L, q_1, q_2) + U_{\text{Coul}}(L, q_1, q_2),$$

its partial derivatives $\partial U / \partial L$, $\partial U / \partial q_i$ and the functions $w_i(L, q_1, q_2)$ have been calculated for the system formed by approaching ^{40}Ar and ^{208}Pb nuclei using the generalized surface potential of ref. [19] in the form of a folded Yukawa plus exponential interaction:

$$U_{\text{folded}} = \frac{c_s}{8\pi^2 a^4 r_0^2} \int_{V_i} d^3 \mathbf{r}_1 \int_{V_j} d^3 \mathbf{r}_2 \left(2 - \frac{\sigma}{a} \right) \frac{\exp(-\sigma/a)}{\sigma/a} \quad (43)$$

with the parameters c_s and a taken from ref. [19]. For the Coulomb part of the potential, the homogeneous charge distribution within the spheroidal droplets with sharp surfaces is assumed:

$$U_{\text{Coul}} = \frac{Z_i Z_j e^2}{2} \int_{V_i} d^3 \mathbf{r}_1 \int_{V_j} d^3 \mathbf{r}_2 \frac{1}{\sigma}. \quad (44)$$

In eqs. (43) and (44) $\sigma = |\mathbf{r}_{1,2}|$ is the distance between the points \mathbf{r}_1 and \mathbf{r}_2 .

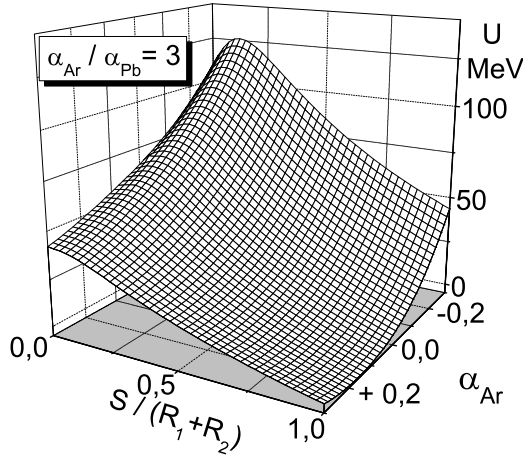


Fig. 1. Potential function $U(L = L_{\text{cont}} + S, \alpha_{\text{Ar}}, \alpha_{\text{Pb}})$ for the ratio $\alpha_{\text{Ar}}/\alpha_{\text{Pb}} = 3$ as a function of α_{Ar} and the distance between the ion surfaces S .

This potential has been tested in different mass regions giving a rather satisfactory description of different phenomena including heavy-ion elastic collisions, fusion and fission. The calculations reported in ref. [19] show, in particular, that the ^{248}Fm nucleus, which is one of possible products of the $^{40}\text{Ar} + ^{208}\text{Pb}$ reaction, has a shallow fission valley with a barrier of about 3 MeV.

Expressions (43) and (44) are used in our study to calculate the potential energy produced by the nuclear and Coulomb interactions within the same ion and the interions interaction potential, taking in an appropriate way the volumes V_i, V_j , and the numbers of protons Z_i, Z_j . We use the technique of ref. [20] based on the Ostrogradsky-Gauss theorem to convert the volume integrals into the surface integrals. For the axially symmetric shapes considered in the paper we finally obtain threefold integrals instead of double-volume integrals.

The potential energy of the model considered here depends on three variables, which introduces some difficulties in its visualization. Figure 1 shows the potential energy surface for the ratio of deformation parameters $\alpha_{\text{Ar}}/\alpha_{\text{Pb}} = 3$ which is close to the one found in the calculations describing the collisions of Ar and Pb at the near-barrier energies (see next section). In the figure the potential is presented as a function of α_{Ar} and of the distance between the surfaces of the ions $S = L - L_{\text{cont}}$, where

$$L_{\text{cont}}(\alpha_{\text{Ar}}, \alpha_{\text{Pb}}) = \frac{R_{\text{Ar}}}{(1 - \alpha_{\text{Ar}})^2} + \frac{R_{\text{Pb}}}{(1 - \alpha_{\text{Pb}})^2}. \quad (45)$$

From this figure one sees a dominant role of the Coulomb repulsion at large distances between the surfaces of ions and the drastic changes in the potential energy produced by the nuclear interaction when S becomes small. The picture shows the “ridge” where

$$\left(\frac{\partial U}{\partial \alpha_{\text{Ar}}} \right)_{L, \alpha_{\text{Pb}}} = \left(\frac{\partial U}{\partial \alpha_{\text{Pb}}} \right)_{L, \alpha_{\text{Ar}}} = 0. \quad (46)$$

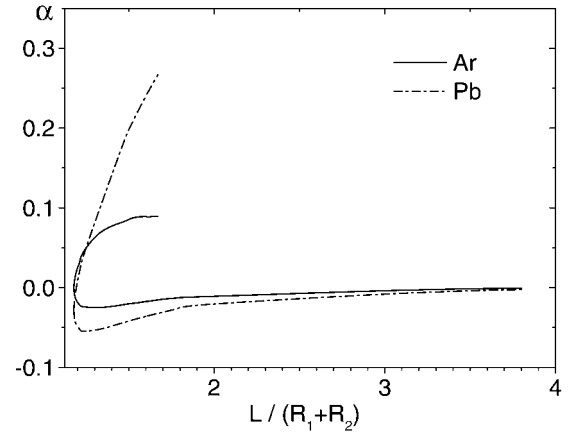


Fig. 2. Lines of zero value of partial derivatives of the potential in α_{Ar} (solid line) and in α_{Pb} (broken line) as a function of $L/(R_1 + R_2)$.

The ridge is situated at the boarder of the compact configuration space. One sees that, with the increase of prolate deformation, the potential energy at the ridge decreases, and that the ridge flattens and gives way to the saddle point.

The deformation parameters found from eq. (46) are shown in fig. 2 in their dependence on L ; in this and in the following figures L is given in the units of $(R_{\text{Ar}} + R_{\text{Pb}})$. In the interval $1.178 < L < 1.5$ each curve has two branches. The deformation parameters for the lower branches are very small, decreasing asymptotically as L^{-3} when L increases. Thus, the lower branch is close to the line of the lowest potential energy of two very rigid ions.

Near the point $L = 1.178$, where the branches join, the nuclear interaction becomes dominant, and the potential energy is the lowest in configurations with a strong prolate deformation. These configurations are represented in the upper branch of the curves. All along this branch Ar ions have prolate deformations, and the Pb ions become prolate at L -values a little bit larger than at the point where the branches join. Along the upper branch the distance between the surfaces of the ions (S) is very small and decreases with the increase of deformation parameters accompanied by the increase of L_{cont} . At the end of this branch the solution of eq. (46) approaches the domain of compact configurations where the matter of two ions is overlapping. Note, that the deformation of Pb is much more pronounced than that of Ar in both branches of solutions of eq. (46).

In fig. 3 the partial derivative $|(\partial U/\partial L)_{\alpha_1, \alpha_2}|$ at the ridge is shown. It decreases along the upper branches of the curves presented in fig. 2 when S decreases. The configuration in which

$$\left(\frac{\partial U}{\partial \alpha_1} \right)_{L, \alpha_2} = \left(\frac{\partial U}{\partial \alpha_2} \right)_{L, \alpha_1} = \left(\frac{\partial U}{\partial L} \right)_{\alpha_1, \alpha_2} = 0 \quad (47)$$

corresponds to the “saddle” in the potential energy surface forming a barrier in the L -direction and a valley in the direction of α_{Ar} and α_{Pb} . These relations are satisfied when $\alpha_{\text{Ar}} \simeq 0.08$, $\alpha_{\text{Pb}} \simeq 0.3$ and $L \simeq L_{\text{cont}} \simeq 1.72(R_{\text{Ar}} + R_{\text{Pb}})$.

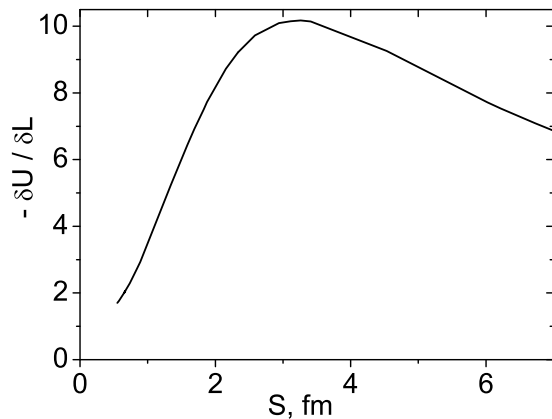


Fig. 3. Partial derivative ($\partial U/\partial L$) at the “ridge” as a function of S .

4 Trajectories of colliding nuclei

The equations of motion have been integrated numerically for the case of $^{40}\text{Ar} + ^{208}\text{Pb}$ central collision, and the time dependence of each of the collective variables has been found. The ensemble of these data determines “the system’s trajectory in the collective phase space”. The trajectories have been studied for several values of the incident energy (E_0).

The conditions of forming a long-living (stationary) state before the contact have been examined in this way. The solutions of dynamical equations fall into two categories: first, describing the quasi-elastic scattering (low energies) and second, corresponding to the formation of compact configurations (higher energies). In the solutions of the first category $L \rightarrow \infty$ when $t \rightarrow \infty$. To be associated with the formation of a stationary state, the asymptotic dependence of the L variable with time must change: it must tend to a certain finite value at $t \rightarrow \infty$. The stationarity conditions of a state follow from eqs. (9), (10), (28) after throwing from them all terms containing the time derivatives. Then, from eq. (28) one finds that in the stationary state $\pi_1 = \pi_2 = 0$. In this case eq. (10) says that $w_{\text{Ar}}(L, q_1, q_2) = w_{\text{Pb}}(L, q_1, q_2) = 0$ and from eq. (21) one deduces that eq. (46) is satisfied. Finally, from eq. (9) it follows that in the stationary state the partial derivative of the potential in L also vanishes. These relations define the configuration where the potential has a stationarity point. Naturally, they are satisfied in the lowest-energy (heated) state. They are equally well satisfied in the local pits in the potential surface, and also at the saddle points of the potential. The trajectory stops reaching each of such points. This may happen at several values of incident energies of colliding ions leading to reactions of different types. The lowest in the energy stationarity point, at which the approaching nuclei arrive, is of course, the saddle point found in our analysis of the potential energy surface.

The calculations show that at energies smaller than 4.92 MeV/n (196.8 MeV incident energy in the laboratory frame) no contact between the nuclei is established. The larger energies correspond to events at which the ions overcome the potential energy ridge and come to a contact

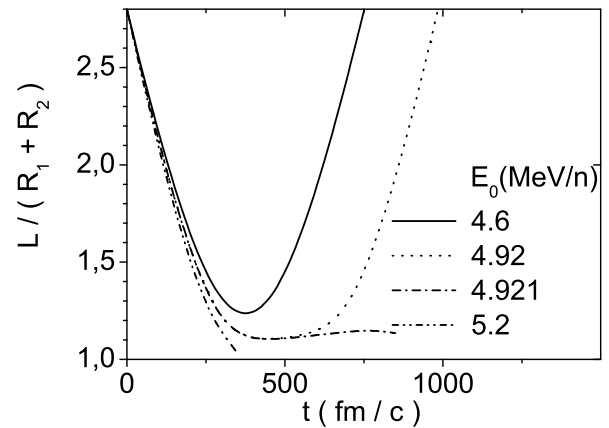


Fig. 4. Distance $L(t)$ for 4 different values of the incident energy E_0 (MeV/n).

forming the compact $Z, A = 100, 248$ nuclear system. In the case of fusion this corresponds to formation of Fermium isotopes. For a systematic study of the dynamics in compact configurations an extension of the theoretical model is needed⁴. Thus, we stop calculations at the moment when the contact between the ions is established. Nevertheless, the material of the paper allows to draw some conclusions concerning the outcome of collisions in which the contact between the ions is established.

In fig. 4 the curves $L(t)$ are presented. One can see that for energies smaller than 4.92 MeV/n the time dependence of $L(t)$ is very close to that found in the elastic Coulomb scattering of nuclei (see the curve for $E_0 = 4.6$ MeV/n). When $E_0 = 4.92$ MeV/n the colliding ions slow down in their approach and rest for some time at practically constant distance without establishing a compact configuration. As in the elastic scattering at lower energies, L increases after reaching a minimum. A very little increase in E_0 changes the trajectory: after passing for some time at a practically constant value of the elongation parameter, the ions come to contact (see the curve for $E_0 = 4.921$ MeV/n).

An exceptional character of the curves corresponding to the energies $E_0 = 4.92$ and $E_0 = 4.921$ MeV/n is evident: these two curves are the closest to the “separatrix” trajectory separating the “quasi-elastic” from the “fusion” events. As it was shown before, the separatrix “stops” at the saddle point where the two ions are strongly deformed and touch each other. The relation between the deformation of the ions (α_{Ar} and α_{Pb}) and the elongation parameter $L(t)$ at the trajectory corresponding to the incident energy $E_0 = 4.92$ MeV/n is shown in fig. 5. In contrast with the properties of the potential energy valley, the deformation of ^{208}Pb on the trajectories remains much lower than that of ^{40}Ar (compare figs. 2 and 5). This feature is explained by the larger inertia of the ^{208}Pb nucleus compared with the inertia of its reaction partner ^{40}Ar .

⁴ This extension is necessary to determine the properties of the “window” contribution to the energy dissipation and the “driving forces” along the mass asymmetry degree of freedom. The study of these problems is underway.

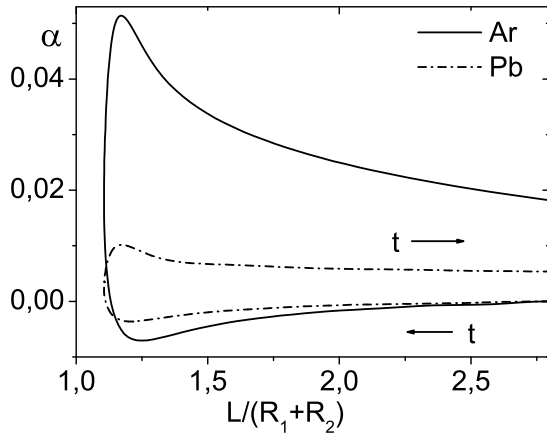


Fig. 5. Trajectory of Ar (solid line) and of Pb ions (broken line) in the α - L plane in the collision at $E_0 = 4.92$ MeV/n. Arrows beside the lines indicate the time evolution.

The figures presented before give an impression of the time scales involved in the nuclear approach at near-barrier energies: typically, the ions pass less than 10^{-22} s within the range of nuclear interaction before hitting each other. This time interval is of the same order of magnitude as the mean relaxation time. The Coulomb scattering at the energies shown in the figures proceeds also very fast. The short duration of this part of approach makes impossible the creeping motion along the valley in the potential energy. Thus the trajectories remain far away from the saddle point configuration. Indeed, the maximal values of deformation parameters attained before coming into the contact in collisions with the energies $E_0 = 4.92$ and $E_0 = 4.921$ MeV/n are much lower than the deformation parameters at the saddle point (see fig. 5). This means that the ions arrive at the saddle point after overcoming the ridge in the potential energy surface, establishing a contact and making a rebound to approach the saddle point from the side of compact configurations.

Such conclusion is in accordance with the results of ref. [3] in which the “elastoplastic” nuclear model operating with only one “geometrical” collective coordinate was applied for the nuclear fusion study in compact configurations. In this paper it was shown that the intrinsic collective energy accumulated just after the contact is sufficiently large to prevent the fusion of the ions if no extra push energy is provided to them to overcome by an appreciable amount the potential barrier. It must be noted, however, that these results are obtained within a very restrictive approximation for the nuclear shape. They have shown, however, that the Fermi surface deformation constitutes one of the origins of the extra push.

In figs. 6a), b) the deformation parameters α_{Ar} , α_{Pb} and the quantities π_{Ar} , π_{Pb} are shown as functions of the time for the collision at $E_0 = 4.92$ MeV/n. The fast variations of these quantities take place during a time interval of the order of 10^{-22} s which is comparable with the mean relaxation time τ . The variations of α_i and π_i are in opposite phases showing that the Fermi surface deformations

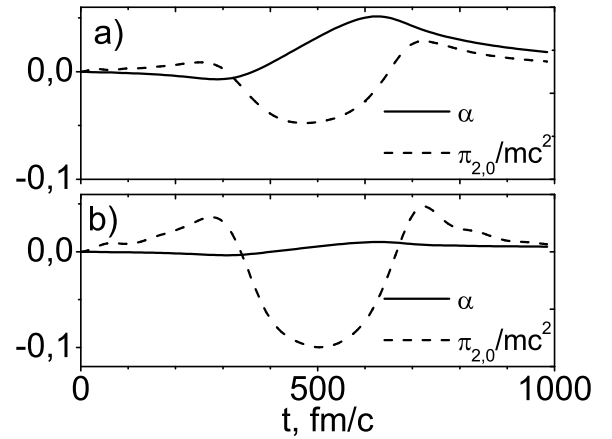


Fig. 6. Time dependence of α and π (in units of mc^2) in the collision at $E_0 = 4.92$ MeV/n. a) for ^{48}Ar , b) for ^{208}Pb .

have the character of elastic vibrations and are not the consequences of the “viscous” flow.

5 Energy dissipation

The deformation of ions leads to the dissipation of collective energy interpreted here as its transformation into the energy of statistical excitation (E_{stat}). It may be found, either by summing the terms in eq. (26), or by integrating in time eq. (35). Both procedures have been used in order to control the accuracy of the results. The second way is found to be preferable for computational reasons.

In fig. 7 the statistical energy accumulated in the scattering in the system of Ar and Pb nuclei (E_{stat}) is shown as a function of the incident energy. For $E_0 \leq 4.92$ MeV/n the statistical energy presented here includes the contribution corresponding to the recoil phase. For larger energies, the values for E_{stat} accumulated up to the moment of the contact are given. The statistical excitation energy

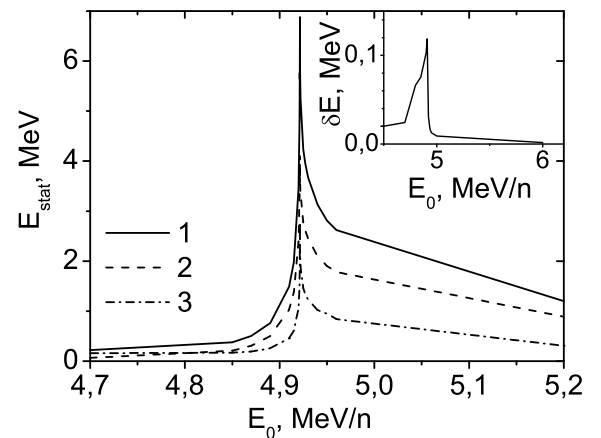


Fig. 7. Statistical excitation energy $E_{stat,i}$ as a function of the incident energy E_0 , ($i = 1, 2, 3$ standing, respectively, for $E_{stat, Ar+Pb}$, $E_{stat, Ar}$ and $E_{stat, Pb}$); in the insert the energy δE_{Ar+Pb} dissipated via GDR excitation in Ar and Pb.

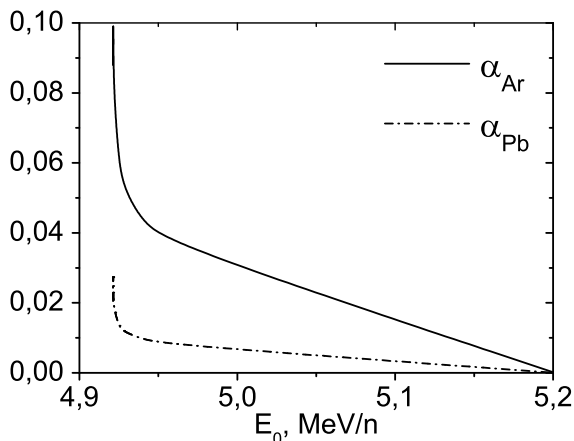


Fig. 8. Deformation parameters α_{Ar} (solid line) and α_{Pb} (broken line) at the moment of contact as a function of E_0 .

is peaked in the collisions with the incident energy close to $E_0 = 4.92$ MeV/n, where its sum in the two ions is equal to 6.5 MeV. As a consequence of the difference in the deformation amplitudes of two ions the lighter partner (Ar) is relatively more “heated” than the heavier (Pb) ion⁵. In the insert of fig. 7 the contribution to the statistical excitation energy from the isovector dipole mode in both ions ($\delta E_{\text{Ar+Pb}}$) is shown. One can see that it is much smaller than the contribution coming from the excitation of the quadrupole modes.

The fast rise of the dissipated collective energy with the incident energy when E_0 is lower than needed for establishing the contact (in the considered case up to $E_0 = 4.92$ MeV/n) does not call for any discussion: the greater is the energy in this domain, the closer is the approach of the ions and the stronger is their mutual interaction. The decrease of the deformation of ions at the moment of contact and of the statistical excitation energy, accumulated before it with the increasing incident energy above this value, is due to the retardation in the “information” transmission between different degrees of freedom during the evolution of the system. The nucleus-nucleus interaction depends on the elongation parameter L . The collective energy dissipates when the changes in L are transmitted to the dynamics of the deformation parameters q_{Ar} and q_{Pb} and then from q_i to π_i . To influence the evolution of L , the transmission of signals of changes in the state of the system in one direction must be followed by the passage of corresponding signals in the opposite direction. Such retardation effects are present even when the relaxation in the momentum space is fast and the viscous approximation can be used [21]. However, the deformation of the Fermi surface makes this passage longer, accentuating the phenomena related with them.

The importance of the retardation increases with the velocity of the ions at the moment of the contact (*i.e.* with E_0) explaining the decrease of the dissipated energy and also the decrease of the deformation of ions acquired before

⁵ The same feature of the evolution of fusing nuclei in the compact configurations is reported in ref. [2].

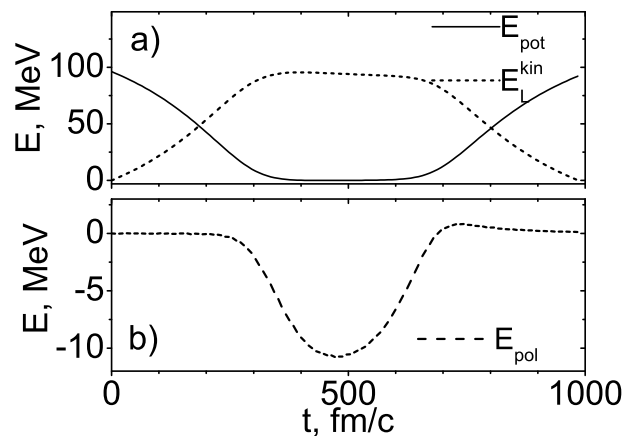


Fig. 9. a) Potential energy $E_{\text{pot}}(t)$ (solid line) and the part of kinetic energy $E_L(t) = \mu\dot{L}^2/2$ (broken line); b) the polarization energy $E_{\text{pol}}(t)$. Here and in fig. 10 the energies are given for the trajectory with $E_0 = 4.92$ MeV/n.

the contact when the incident energy increases more than needed to overcome the threshold for the contact [21]. The dissipated energy is the largest in the trajectories close to the “separatrix”: see fig. 8, which shows the deformation of ions at the point of contact as the function of the incident energy. So, in the study of events at the energies substantially higher than the minimal needed for establishing the contact of ions, their deformation before the contact is of minor importance.

Within the model the saddle point energy may be estimated as the potential energy met by the colliding ions at the plateau of the “exceptional trajectories”. The potential energy along the trajectory corresponding to $E_0 = 4.92$ MeV/n as a function of time is shown in fig. 9a) together with the kinetic energy of relative motion $E_L = \mu\dot{L}^2/2$. The plateau in the time interval from 400 fm/c to 600 fm/c is clearly seen here. The effective barrier met by the colliding ions, estimated by the data corresponding to this trajectory, is equal to $E_0^{\text{c.m.}} - E_{\text{stat}} = 158.6$ MeV ($E_0^{\text{c.m.}} = 165.1$ MeV being the incident energy in the center-of-mass reference frame).

More information on the dynamics of the system is contained in fig. 9b). Here the potential energy of polarization of ions is shown:

$$E_{\text{pol}} = E_{\text{pot}} - \frac{Z_{\text{Ar}}Z_{\text{Pb}}e^2}{L(t)} - E_{\text{pot}}(L \rightarrow \infty).$$

The subtraction from the potential energy of the bulk of the long-range Coulomb interaction and of the intrinsic energy of separated ions changes drastically the outlook of the curve: the plateau disappears giving way to a rather well pronounced minimum (at which $E_{\text{pol}} = -10.7$ MeV). The figure shows that on the trajectory with $E_0 = 4.92$ MeV/n the ions remain in the range of nuclear forces for only a very limited time (about $2 \cdot 10^{-21}$ s). Thus, the separatrix corresponds to somewhat larger incident energies and the height of the effective potential barrier is somewhat larger than quoted above.

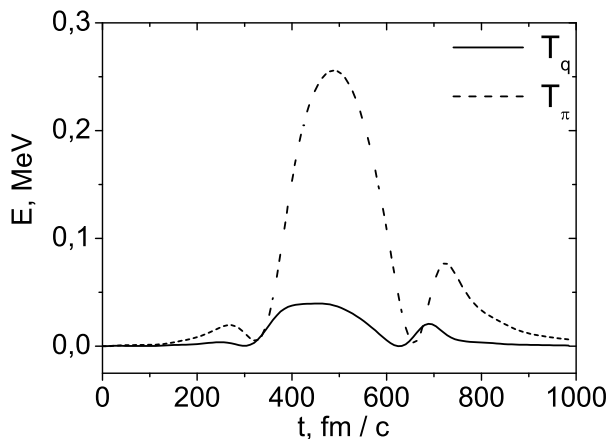


Fig. 10. Kinetic energy of collective flow T_q (solid line), and energy of the Fermi surface deformation T_π (broken line).

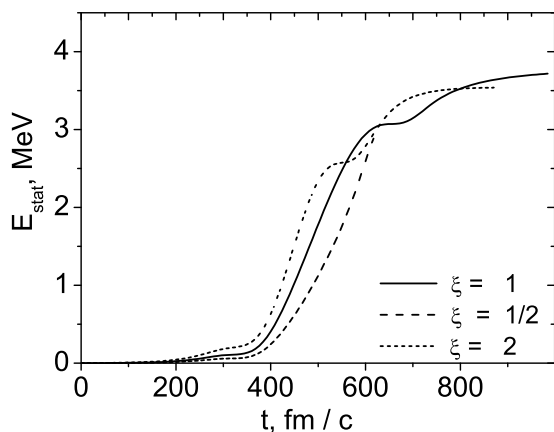


Fig. 11. Total statistical excitation energy as a function of time for three different values of the relaxation time parameter τ . The values of τ are given by ξ (see eq. (41) and the text after eq. (42)).

In the region of the plateau in the potential energy, the kinetic energy of translations $\mu\dot{L}^2/2$ is very small. From fig. 10 one finds that the same is true for the kinetic energy of the intrinsic collective motion within the ions $T_q = T_{q_{Ar}} + T_{q_{Pb}}$. The intrinsic energy of the Fermi surface deformation $T_\pi = T_{\pi_{Ar}} + T_{\pi_{Pb}}$ turns out to be an order of magnitude greater than T_q .

In fig. 11 the statistical excitation energy E_{stat} attained during the approach is shown as a function of time for 3 different values of the relaxation time parameters τ . The values of τ are given by the parameter ξ in eq. (41). The value $\xi = 1$ is used in the bulk of calculations presented before; in the adiabatic regime it corresponds to the “wall” friction parameter of ref. [2]. With the value $\xi = 2$ the systematics on the widths of GQR (see ref. [18]) is reproduced. The value $\xi = 1/2$ corresponds to half of the wall formula friction parameter. One sees that the differences in E_{stat} at the contact point are very small. Equally modest sensitivity to the value of τ is found for the other characteristics of trajectories.

The general tendencies of the collective energy dissipation in the Ar + Pb system are the same as reported in ref. [5] for the collision in a symmetrical Mo + Mo system. In particular, close values of the maximal statistical excitation energy acquired before the collision in the two systems are found.

It is a commonly used practice to associate the collective energy dissipation with the frictional forces proportional to the time derivatives of deformation parameters. Then, the rate of collective energy decrease is given by the quadratic function of \dot{q}_i . As shown before, this substitution is reasonable when the evolution is slow and π_i are proportional to \dot{q}_i . Figure 5 and fig. 8 show that the proportionality of π_i and \dot{q}_i functions is lost when the ions approach so much that the nuclear interaction becomes important: it introduces rapid changes in the shape variations, and the retardation effects associated with the Fermi surface deformation become important.

There is much uncertainty in the values of the friction parameters compatible with the relevant experimental data [21]. To reconcile the adiabatic theory with experimental information one introduces the excitation energy or/and the shape dependence of the friction force. We have found that this technique is nothing but the simulation of a more involved collective dynamics in which the elastoplastic properties of nuclei are included.

6 Summary and conclusions

The dynamical effects produced by spheroidal deformations of approaching heavy ions experiencing the central collision are discussed in this paper in the framework of a model in which the configurations of the system are defined by three independent coordinates: the distance between the center of mass of ions and their quadrupole moments. Such parametrization encompasses the close-to-spherical shapes of the ions typical for the approach phase in the heavy-ion collision and also very deformed shapes of the ions which could be met in the case of nuclear fission.

The potential energy dependence on the collective coordinates is evaluated by summing the contributions of Coulomb and nuclear interactions. The latter contribution is found by using the folding procedure applied to the Yukawa + exponential interaction.

The model takes in account the “memory effects” which are associated with deformations of the Fermi surface. The quantities measuring the Fermi surface deformation are treated as kinematically independent generalized velocities. This allows to write the equations of motion in the canonical form of Lagrange-Rayleigh classical mechanics. It is done in extending the collective space by including into it the coordinates associated with the distribution of nucleons in the momentum sector of the phase space. This makes the model equivalent to the “transport theory” approaches of nuclear dynamics defined in an extended space of coordinates.

One of the advantages of such a formulation is that it does not contain any ambiguity in the estimation of the collective energy transformed into the energy of statistical

excitation. Another advantage lies in the easy access to the treatment of fluctuations of collective observables [5]. This possibility has not yet been fully exploited waiting for our study (in progress) of the whole process of fusion including the evolution in the compact configuration formed by the colliding nuclei.

Let us recapitulate the main results obtained in this way:

- The properties of the 3-dimensional potential energy surface have been examined. The saddle-like configuration is found lying on the border of compact configurations formed by very deformed ions.
- The study shows the role of the inertia forces. Due to them the trajectories of the fusing system do not follow the valley in the potential energy surface. This effect is pronounced more in the motion of the heavier ion than in the motion of its lighter partner.
- The estimation is done of the amount of dissipated collective energy during the approach and compared with the potential energy decrease due to the polarization of ions. For the reaction $^{40}\text{Ar} + ^{208}\text{Pb}$ the two effects nearly compensate each other.
- The polarization of ions via excitations of the isovector dipole mode is also examined but found to be very small.
- The combined effect of the polarization and dissipation of the collective energy during the approach diminishes the energy needed for establishing the contact between the ions by about 4 MeV. However, the “separatrix” trajectory, at which the unification of ^{40}Ar and ^{208}Pb nuclei becomes possible, corresponds to the collision energies greater than needed for establishing the contact between them.

The microscopically determined potential energy surfaces possess numerous saddle point configurations corresponding to different overlaps of colliding ions. The potential energy in the saddle point discussed in the paper may be regarded as a barrier for the formation of the composite system with the lifetime sufficient for the equilibration in the motion of individual nucleons.

The fusion becomes possible if the trajectories surpassing this saddle point are not stopped before reaching the other saddle points. If not, the reactions different from the fusion (*e.g.*, quasi-fission) will take place at energies lower than necessary for surpassing other saddle points. One may say that in general each type of reaction demands different amount of an extra push energy. This remark recalls the experimentally found difference in the outcomes of $^{48}\text{Ca} + ^{238}\text{U}$ and $^{48}\text{Ca} + ^{244}\text{Pu}$ reactions: the quasi-fission is observed at an energy lower by about 10 MeV than needed for the formation of the $Z = 112$ and $Z = 114$ compound nuclear systems [1].

We think that the formalism presented here will be useful in the future theoretical investigations in this domain for studying the problems left outside of consideration here: for the treatment of the all possible sources of dissipation, for learning more about the “window friction” and about the driving forces in the mass asymmetry collective coordinate etc.

Appendix A. Quantum substratum of the approach

Equations (24) determining the collective part of the zero-point kinetic energy and the intrinsic collective variables ζ_i are an heritage of the quantum (many-fermionic) nature of nuclei.

One comes to the relations (24) using the results of refs. [22, 23] from which it follows that in the diabatic (opposite to the “viscous”) regime, when the dissipation is absent, the quantity

$$\Omega_3^{(i)} \equiv \left(m^3 V_i^2 \prod_{\mu=1}^3 \Pi_{\mu,\mu}^{(i)} \right)^{1/6}$$

is an invariant of motion. This quantity, having the dimension of the Planck unit \hbar , represents the volume occupied by the nucleus in the 6-dimensional phase space of one particle. Its conservation is inherent in the Hartree-Fock theory in which the wave function is approximated by a single Slater determinant containing time-dependent one-particle functions. In the quantum description the configuration mixing is caused by the correlation term and appears in the approach of this paper in the form of the collision integral. The conservation of $\Omega_3^{(i)}$ is established in [22] using the virial theorems approach and also in ref. [23] where it is deduced on the basis of more sophisticated mathematical technique (both papers deal with the motion including the rotational currents and present the invariant in a more general form). When the differences between the quantities $\Pi_{\mu,\mu}^{(i)}$ corresponding to different μ values are small and the volume V_i is fixed one arrives at eq. (24) expanding $\Pi_{\parallel}^{(0)}$ in a Taylor series in

$$\frac{\Pi_{\parallel}^{(i)} - \Pi_{\perp}^{(i)}}{\Pi_{\parallel}^{(i)} + \Pi_{\perp}^{(i)}}$$

at a fixed value of $\Omega_3^{(i)}$.

The quantum counterpart of ζ_i is the “shift operator” transforming one intrinsic state into another. The quantum states involved in the dissipation correspond to different values of $\Omega_3^{(i)}$ and lie in the region of energies around the centroid of the GQR. The density of quantum levels here is extremely high, and the proposed classical treatment of quantum properties seems to be justified.

Appendix B. Renormalization of the mean relaxation time

Note that in the derivation of β_i^{wall} only the “one-body” dissipation effects are included. The mean relaxation time approximation, used in the paper, considers the dissipation as being produced by the collisions of nucleons, *i.e.* has rather a two-body origin leading directly to the equilibration in the distribution of nucleons in the momentum

space. It affects the collective motion by its coupling with the intrinsic motion. The inclusion into the theoretical scheme of other than q_i global collective variables (such as the higher multipole moments in the matter distribution) involves additional nuclear characteristic depending on the distribution of nucleons in the momentum space (see refs. [8,9]). This in turn introduces additional terms in the dissipation function. Hopefully, they could be accounted for by re-normalizing the mean relaxation time parameters τ_i .

Among the other global nuclear characteristics the octupole moment in the matter distribution seems to be of a particular importance. It is related with the mass asymmetry whose evolution is found to be of an utmost importance for the outcome of the heavy-ion collision. Considering here only the phase of approach, when the “window” between the ions is closed and the asymmetry degree of freedom is frozen, we leave for future studies the inclusion of this degree of freedom into the model.

One of the authors (IM) acknowledges the hospitality of the CSNSM (Orsay) where an important part of his contribution to this work has been done during his visits to France in the framework of the JINR-IN2P3 Collaboration agreement. We address our thanks to Prof. Yu.Ts. Oganessian, Prof. M. Di Toro, Prof. P. Quentin for numerous illuminating discussions.

References

1. Yu.Ts. Oganessian *et al.*, Phys. Rev. C **70**, 064609 (2004).
2. J.P. Blocki, H. Feldmeier, W.J. Swiatecki, Nucl. Phys. A **459**, 145 (1986).
3. I.N. Mikhailov *et al.*, Nucl. Phys. A **604**, 358 (1996).
4. I.N. Mikhailov *et al.*, Nucl. Phys. A **641**, 64 (1998).
5. T.I. Mikhailova *et al.*, Part. Nucl. Lett. **1**, 13 (2002).
6. S. Chandrasekhar, *Ellipsoidal Figures of Equilibrium* (Dover, New-York, 1987).
7. I.N. Mikhailov, Part. Nucl. **31**, 838 (2000).
8. E.B. Balbutsev, I.N. Mikhailov, *Collective Nuclear Dynamics*, edited by R.V. Djolos (USSR Academy of Sciences Publ., Leningrad, 1990).
9. E.B. Balbutsev, Part. Nucl. **22**, 333 (1991).
10. E. Wigner, Phys. Rev. **40**, 749 (1932).
11. Å. Bohr, B. Mottelson, *Nuclear Structure*, Vol. **1** (World Scientific, 1998) Chapt. 2A-7.
12. R. Balescu, *Equilibrium and Nonequilibrium Statistical Mechanics*, Vol. **2** (Wiley-Interscience Publ., New York, 1975) Chapt. 12.
13. P. Résibois, M. De Leener, *Classical Kinetic Theory of Fluids* (Wiley-Intersciences Publ., New York, 1977).
14. H. Goldstein, *Classical Mechanics*, 2nd edition (Addison-Wesley Publ. Comp., 1980).
15. E.B. Balbutsev, I.N. Mikhailov, J. Phys. G **14**, 545 (1988).
16. Å. Bohr, B. Mottelson, *Nuclear Structure*, Vol. **2** (World Scientific, 1998).
17. J. Blocki *et al.*, Ann. Phys. (N.Y.) **113**, 330 (1978).
18. M.N. Harakeh, A. van der Woude, *Giant Resonances: Fundamental High Frequency Modes of Nuclear Excitation* (Oxford University Press, Oxford, 2001).
19. H.J. Krappe, J.R. Nix, A.J. Sierk, Phys. Rev. C **20**, 992 (1979).
20. K.T.R. Davies, J.R. Nix, Phys. Rev. C **14**, 1977 (1976).
21. Y. Abe *et al.*, Phys. Rep. **275**, 49 (1996).
22. I.N. Mikhailov *et al.*, *Quantum Riemann rotating ellipsoids*, in preparation.
23. M. Cerkaski, I.N. Mikhailov, Ann. Phys. **223**, 151 (1993).